

# Folding Mechanism of Small Proteins

Seung-Yeon Kim<sup>1</sup>, Julian Lee<sup>1,2</sup>, and Jooyoung Lee<sup>1\*</sup>

<sup>1</sup>*School of Computational Sciences,*

*Korea Institute for Advanced Study, Seoul 130-012, Korea*

<sup>2</sup> *Department of Bioinformatics and Life Sciences,*

*Soongsil University, Seoul 156-743, Korea*

## Abstract

Extensive Monte Carlo *folding* simulations for four proteins of various structural classes are carried out, using a *single* atomistic potential. In all cases, collapse occurs at a very early stage, and proteins fold into their native-like conformations at appropriate temperatures. The results demonstrate that the folding mechanism is controlled not only by thermodynamic factors but also by kinetic factors: The way a protein folds into its native structure, is also determined by the convergence point of early folding trajectories, which cannot be obtained by the free energy surface.

PACS numbers: 87.14.Ee, 87.15.-v, 05.20.Dd, 05.70.-a

---

\* correspondence to: jlee@kias.re.kr

Understanding how a protein folds is a long-standing challenge in modern science. Computer simulations [1, 2, 3, 4, 5, 6, 7, 8, 9, 10, 11, 12, 13] have been carried out to understand the folding mechanism. However, simulation of protein-folding processes with an atomistic model is a very difficult task. The difficulties come from two sources: (i) Direct folding simulation using an all-atom potential requires astronomical amounts of CPU time, and typical simulation times are only about a few nanoseconds. (ii) Atomic pairwise interactions including solvation effects may not be accurate enough. An extensive folding simulation has been carried out for the villin headpiece subdomain (HP-36), where 1- $\mu s$  molecular dynamics simulation with an all-atom potential has been performed, producing only candidates for folding intermediates [1]. For this reason, direct folding simulations have been mainly focused on simple models, such as lattice models [2, 3], models where only native interactions are included (Go-type models) [4, 5, 6, 7], and a model with discrete energy terms whose parameters are optimized *separately* for each protein [8]. Alternative indirect approaches have also been proposed including unfolding simulations [7, 9, 10, 11] starting from the folded state of a protein. However, it is not obvious whether the folding is the reverse of the unfolding [3, 7]. Moreover, to the best of our knowledge, no one has yet succeeded in folding more than one proteins into their native states using a *single* potential, even with simplified models [8].

In this letter, we propose a novel method to fold several of small proteins using Monte Carlo dynamics. This method uses a *single* atomistic continuous potential which includes *all pairwise* (native and non-native) interactions, and yet allows us to carry out *folding* simulations starting from non-native conformations. We observe that all proteins fold into their native-like conformations at appropriate temperatures. We find that the folding mechanism is controlled by both kinetic and thermodynamic factors [14]: The way a protein folds into its native structure, is determined not only by the free energy surface, but also by the convergence point of early folding trajectories relative to the native state.

We consider a system where an off-lattice potential energy function including non-native interactions is utilized. We study the folding dynamics of proteins using a united-residue (UNRES) [15] force field where a protein is represented by a sequence of  $\alpha$ -carbons linked by virtual bonds with attached united side chains and united peptide groups. Energy terms are all continuous, and include pairwise electrostatic, van der Waals, and multibody terms (see Ref. [15] for details). The effect of solvent was indirectly included in the force field. The

parameters of the UNRES force field were *simultaneously* optimized [16] for four proteins of betanova [11, 17] (20 residues, three-stranded  $\beta$ -sheet), 1fsd [18] (28 residues, one  $\beta$ -hairpin and one  $\alpha$ -helix), HP-36 [1, 12] (36 residues, three-helix bundle), and fragment B of staphylococcal protein A [5, 7, 9, 10, 13, 19] (46 residues, three-helix bundle). The low-lying local-energy minima for these proteins were found by the conformational space annealing [20] method. The parameters were modified in such a way that the native-like conformations are energetically more favored than the others. The global minimum-energy conformations found using the optimized force field are of the root-mean-square deviation (RMSD) values 1.5 Å, 1.7 Å, 1.7 Å and 1.9 Å from the *experimental* structures for betanova, 1fsd, HP-36 and protein A, respectively. After the parameter optimization, *one* set of the parameters is obtained for four proteins.

In the UNRES force field there are two backbone angles and two side chain angles per residue (no side-chains for glycines). The values of these angles are perturbed one at a time, typically about  $15^\circ$ , and the backbone angles are chosen three times more frequently than the side chain angles. The perturbed conformation is accepted according to the change in the potential energy, following Metropolis rule. Since only small angle changes are allowed one at a time, the resulting Monte Carlo dynamics can be viewed as equivalent to the real dynamics. At a fixed temperature, at least ten independent simulations starting from various non-native states of a protein were performed up to  $10^9$  Monte Carlo steps (MCS) for each run. During simulation the values of RMSD from the native structure and the radius of gyration ( $R_g$ ) were calculated using  $C_\alpha$  coordinates. The lowest RMSD values from folding simulations are 0.78 Å, 1.07 Å, 1.58 Å and 2.07 Å for betanova, 1fsd, HP-36 and protein A, respectively. The fractions of the native contacts ( $Q$  and  $\rho$ ) were also measured during simulations, where  $Q$  is calculated from the experimental structure. A native contact is defined to exist when two  $C_\alpha$ 's separated more than two residues in sequence are placed within 7.0 Å. To define  $\rho$  we first characterize the native state conformations by performing simulations starting from the experimental structures, at the same temperatures where folding simulations were performed. We define  $\rho$  as the fraction of native contacts weighted over their contact probabilities in the native state simulations [7, 10, 11]. Due to the fluctuation of the native conformation, the value of  $Q$  is usually lower than that of  $\rho$ .

The time histories of the typical trajectories from the folding simulations of betanova and HP-36 are shown in Fig. 1. The trajectories for 1fsd and protein A are similar to those

in the figure. We observe that collapse occurs at a very early stage ( $\sim 10^4$  MCS) for all four proteins, but the details of each folding process appear to depend on the secondary structure contents. Distributions of RMSD,  $Q$ ,  $\rho$  and  $R_g$  are also accumulated during the whole simulations. The distributions of RMSD are shown in Fig. 2, and those for  $\rho$  and  $R_g$  are shown in Fig. 3 as contour plots. The early folding trajectories plotted in Fig. 3 are obtained as follows. We divided the initial  $10^5$  MCS into 19 intervals (ten  $10^3$  MCS and subsequent nine  $10^4$  MCS), and took average over conformations in each interval. These averages were again averaged over 100 independent simulations starting from random conformations. The same procedure was applied to 100 independent simulations starting from a fully extended conformation.

The simulation of betanova at  $T = 40$  (arbitrary unit) starting from an unfolded conformation demonstrates that rapid collapse occurs in about  $10^4$  MCS; the value of  $R_g$  decreases, whereas the value of  $Q$  remains below 0.3 (Fig. 1). During the next  $10^8$  MCS, more compact states appear, and the value of  $Q$  moves up as high as 1.0. There are two values of RMSD that are populated (see also Fig. 2(b)): one corresponds to less ordered structures (RMSD $\sim 5$  Å) and the other to native-like structures (RMSD $\sim 2.5$  Å). This demonstrates, although the native-like structure is the most stable one, thermal fluctuation can temporarily kick the protein out of the native structure.

We now analyze the details of the folding behavior of each protein. For betanova at low temperatures ( $T \leq 30$ ), the probability distributions of various quantities such as RMSD depend on initial conformations, showing its glassy behavior (Fig. 2(a)). At higher temperatures ( $T \geq 40$ ) this non-ergodic glassy behavior disappears. It should be noted that native-like structures are more easily found from the simulation at  $T = 40$  (Fig. 2(b)) than from the best of ten runs at  $T = 30$ . When temperature decreases from  $T = 80$  to 60, the location of the RMSD peak dramatically moves from 8 Å to 3 Å. This demonstrates the cooperative folding characteristics of betanova. For  $40 \leq T \leq 60$  betanova folds into its native-like structure. The initial folding trajectories and the distribution of  $(\rho, R_g)$  at  $T = 40$  are shown in Fig. 3(a) for betanova. Regardless of its initial conformation (either random or fully extended), the average pathways to the folded conformation initially converge to  $(\rho, R_g) \sim (0.35, 8.5 \text{ Å})$ , and then they move horizontally to the native structure. This is consistent with the recent folding scenario for proteins with  $\beta$  structure [7]. The populated states [11] around  $\rho \sim 0.4-0.5$  and  $R_g \sim 11-12 \text{ Å}$  are not from initial folding trajec-

ories, but from the fluctuation of native-like structures. This kinetic information is difficult to be captured by free energy calculations alone [11].

For 1fsd the distributions of various quantities for ten independent runs ( $10^9$  MCS each) show glassy behavior for  $T \leq 50$ . Again, the non-ergodic glassy behavior disappears at higher temperatures ( $T \geq 70$ ). Fig. 2(c) shows the RMSD distributions at various temperatures. The strength of the cooperativity for 1fsd is not as strong as that of betanova. Again after initial collapse to  $(\rho, R_g) \sim (0.3, 9 \text{ \AA})$ , the average trajectories move horizontally (Fig. 3(b)), although less prominently so compared to the case of betanova.

For HP-36, the distributions of various quantities for ten independent runs ( $10^9$  MCS each) again show glassy behavior at  $T = 60$ . At higher temperatures we have two RMSD peaks (Fig. 2(d)). At  $T = 90$  the peak near the native structure begins to dominate, and as temperature decreases it becomes stronger. This double peak feature demonstrates the cooperative two-state transition. The conformations centered at the higher value of RMSD come from a variety of collapsed states. The conformations from the other peak are native-like. When we examine them, the helix I (residues 4-8) is stably formed [12], while the others are fluctuating. The initial folding trajectories (Fig. 3(c)) converge to  $(\rho, R_g) \sim (0.2, 11 \text{ \AA})$ . These collapsed structures fold into native-like structures  $(\rho, R_g) \sim (0.7, 10 \text{ \AA})$ . Compared to the case of betanova and 1fsd, the average folding trajectories are more diagonal.

The overall folding characteristics of protein A are similar to those of HP-36. The initial folding trajectories (Fig. 3(d)) converge to  $(\rho, R_g) \sim (0.25, 12 \text{ \AA})$ . These collapsed states fold into native-like structures in a diagonal fashion similar to the case of HP-36. When we examine the native-like conformations with  $3 \text{ \AA} \leq \text{RMSD} \leq 4 \text{ \AA}$ , the helix III (residues 42-55) is most stably formed. This is in agreement with recent investigations [9, 13, 19]. We also observe that a first-order like collapse transition [5] (from  $(Q, R_g) \sim (0.15, 18 \text{ \AA})$  to  $(0.15, 12 \text{ \AA})$ ) occurs near  $T = 120$ .

By using an atomistic model, we could observe folding processes of four small proteins in realistic settings. In all cases, rapid collapse is followed by subsequent folding process that takes place in a longer time scale. The folding mechanism suggested in this study is as follows: There are two aspects of folding dynamics, (i) non-equilibrium kinetic properties and (ii) equilibrium thermodynamic properties (Fig. 4). The non-equilibrium kinetic properties, relevant to the early folding trajectories (fast process), can be examined only by direct folding simulations. The free energy surface, an equilibrium thermodynamic property, dictates the

way an initially collapsed state completes its folding (slow process). The way a protein folds into its native structure, i.e., either horizontally or diagonally in  $(\rho, R_g)$  plane, is determined by the position of  $(\rho, R_g)$  where early folding trajectories converge, relative to the native state. It appears that slow folding process of  $\alpha$ -proteins occurs in a diagonal fashion compared to that of proteins containing  $\beta$ -strands [7].

In conclusion, we successfully carried out direct folding simulations of more than one proteins using a *single* atomistic potential. We also observe that glassy transitions occur at low temperatures. The results provide new insights into the folding mechanism.

- 
- [1] Y. Duan and P. A. Kollman, *Science* **282**, 740 (1998).
- [2] J. Skolnick and A. Kolinski, *Science* **250**, 1121 (1990); A. Sali, E. Shakhnovich, and M. Karplus, *Nature (London)* **369**, 248 (1994); H. S. Chan and K. A. Dill, *Proteins* **30**, 2 (1998); D. K. Klimov and D. Thirumalai, *ibid.* **43**, 465 (2001); J. N. Onuchic, Z. Luthey-Schulten, and P. G. Wolynes, *Annu. Rev. Phys. Chem.* **48**, 545 (1997).
- [3] A. R. Dinner and M. Karplus, *J. Mol. Biol.* **292**, 403 (1999).
- [4] N. Go, *Annu. Rev. Biophys. Bioeng.* **12**, 183 (1983).
- [5] Y. Zhou and M. Karplus, *Nature (London)* **401**, 400 (1999).
- [6] O. V. Galzitskaya and A. V. Finkelstein, *Proc. Natl. Acad. Sci. USA* **96**, 11299 (1999); E. Alm and D. Baker, *ibid.* **96**, 11305 (1999); V. Munoz and W. A. Eaton, *ibid.* **96**, 11311 (1999).
- [7] J.-L. Shea and C. L. Brooks, *Annu. Rev. Phys. Chem.* **52**, 499 (2001).
- [8] E. Kussel, J. Shimada, and E. Shakhnovich, *Proc. Natl. Acad. Sci. USA* **99**, 5343 (2002).
- [9] D. O. V. Alonso and V. Daggett, *Proc. Natl. Acad. Sci. USA* **97**, 133 (2000).
- [10] E. M. Boczko and C. L. Brooks, *Science* **269**, 393 (1995).
- [11] B. D. Bursulaya and C. L. Brooks, *J. Am. Chem. Soc.* **121**, 9947 (1999).
- [12] A. Fernandez, M.-Y. Shen, A. Colubri, T. R. Sosnick, R. S. Berry, and K. Freed, *Biochemistry* **42**, 664 (2003).
- [13] A. Ghosh, R. Elber, and H. A. Scheraga, *Proc. Natl. Acad. Sci. USA* **99**, 10394 (2002).
- [14] J. Lee, M. A. Novotny, and P. A. Rikvold, *Phys. Rev. E* **52**, 356 (1995).
- [15] A. Liwo, S. Oldziej, M. R. Pincus, R. J. Wawak, S. Rackovsky, and H. A. Scheraga, *J. Comput. Chem.* **18**, 849 (1997).
- [16] J. Lee, K. Park, and J. Lee, *J. Phys. Chem. B* **106**, 11647 (2002).
- [17] T. Kortemme, M. Ramirez-Alvarado, and L. Serrano, *Science* **281**, 253 (1998).
- [18] B. I. Dahiyat and S. L. Mayo, *Science* **278**, 82 (1997).
- [19] Y. Bai, A. Karimi, H. J. Dyson, and P. E. Wright, *Protein Sci.* **6**, 1449 (1997).
- [20] J. Lee, H. A. Scheraga, and S. Rackovsky, *J. Comput. Chem.* **18**, 1222 (1997).

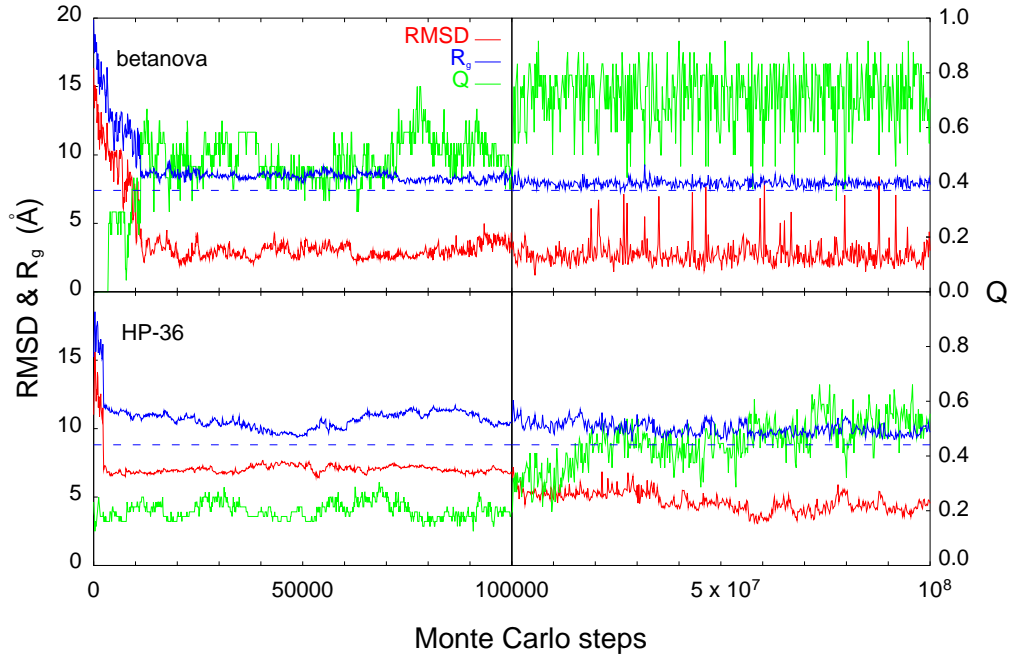


FIG. 1: Typical folding trajectories of betanova at  $T = 40$  and HP-36 at  $T = 70$  starting from non-native conformations. RMSD,  $R_g$  and  $Q$  are plotted for every 100 MCS in the early part and for every  $2 \times 10^5$  steps in the subsequent part. The dotted lines represent the values of  $R_g$  of the native states.



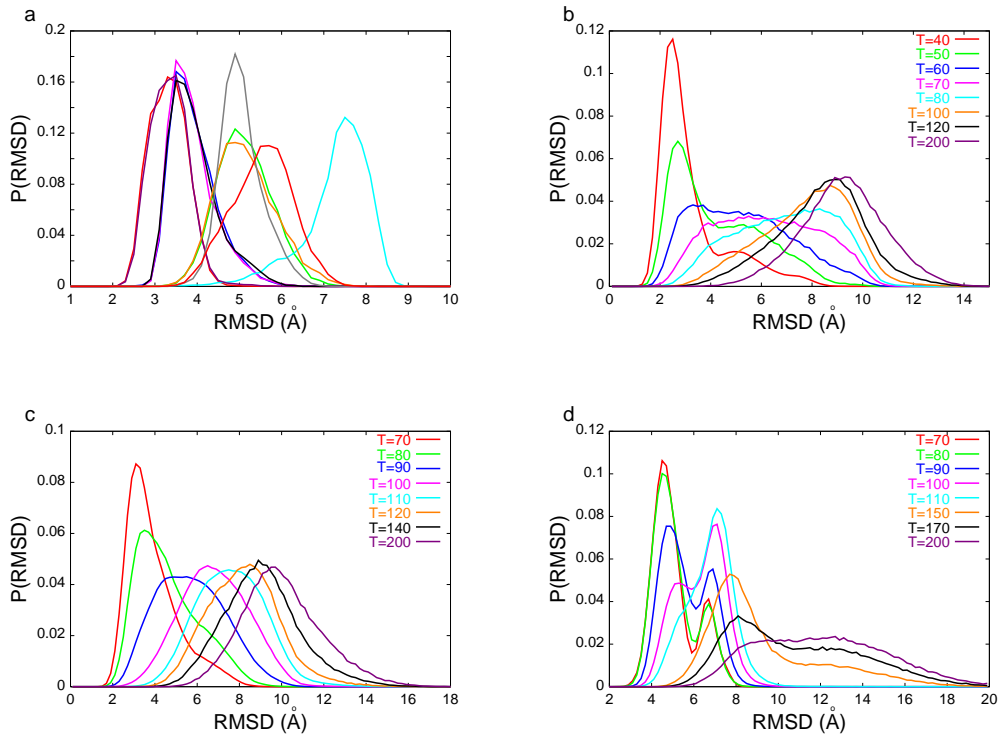


FIG. 2: The probability distributions of RMSD. (a) The distributions of 10 simulations for betanova, starting from random conformations at  $T = 30$ . The glassy behavior is apparent. (b) RMSD distributions of betanova at various temperatures. As temperature decreases, the value of prominent RMSD dramatically moves from 9.0  $\text{\AA}$  to 2.5  $\text{\AA}$ . (c) The distributions for 1fsd. The value of the most probable RMSD drops rapidly from 9.0  $\text{\AA}$  to 3.1  $\text{\AA}$ . (d) The distributions for HP-36. The double peak structure appears for  $T \leq 100$ , representing the cooperative (first-order like) two-state transition.

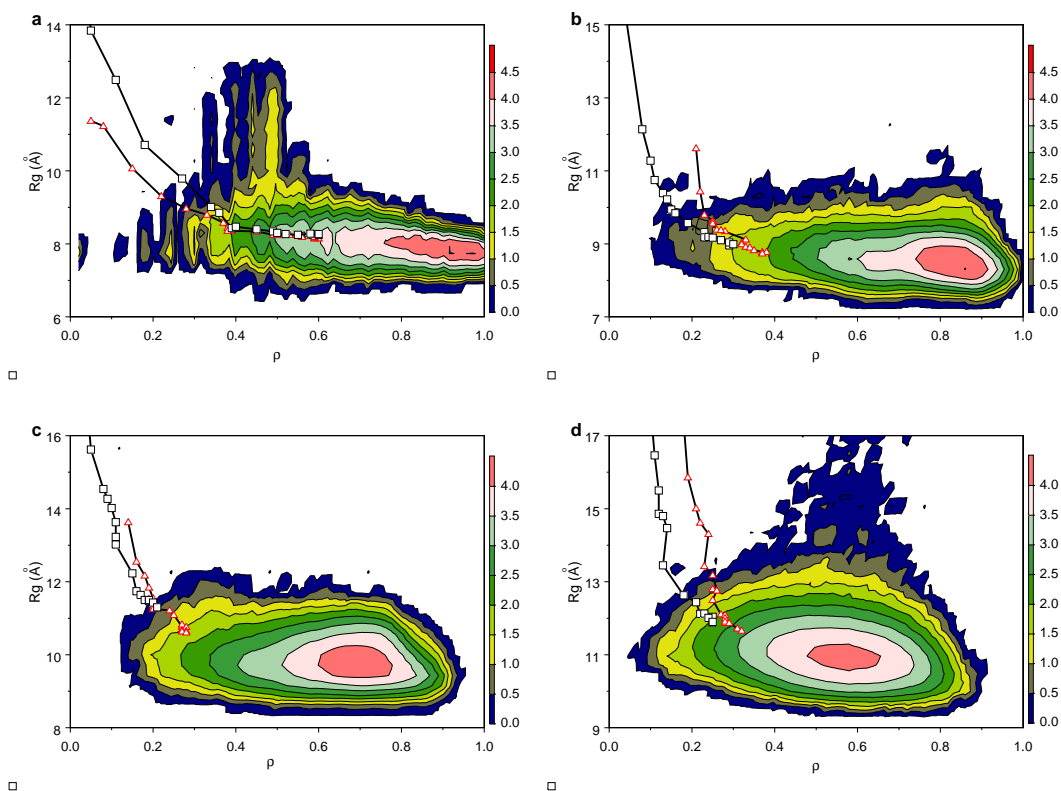


FIG. 3: The initial folding trajectories and the contour plots of the population distributions as a function of  $\rho$  and  $R_g$  at appropriate temperatures. The triangles represent the averages of 100 folding trajectories starting from random conformations. The squares are from 100 trajectories starting from a fully extended conformation. The color scale indicates the exponent  $x$  of the population  $10^x$  at given values of  $\rho$  and  $R_g$ . (a) betanova at  $T = 40$ . (b) 1fsd at  $T = 70$ . (c) HP-36 at  $T = 70$ . (d) protein A at  $T = 80$ .

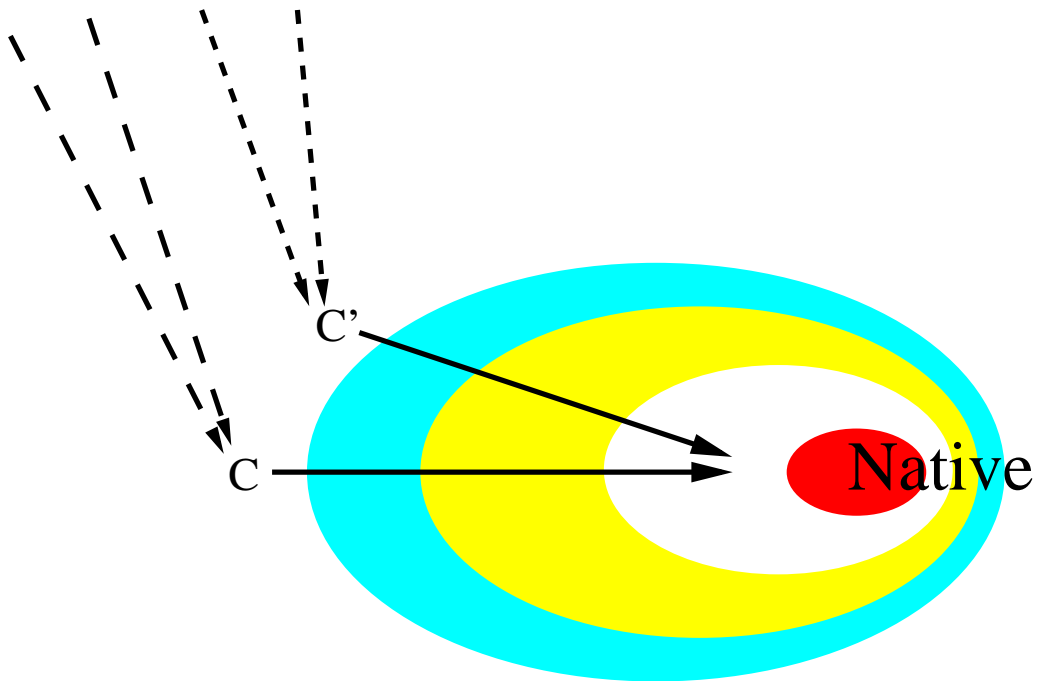


FIG. 4: A schematic of the folding trajectories. The colored contour represents the free energy surface, which is an equilibrium property. Even for proteins with identical free energy landscape, the early folding trajectories (dashed lines) may converge into different points (C or C'). The solid lines represent the later part of the folding trajectories dictated by the free energy landscape. The position of the convergence point of a protein is determined by its kinetic properties. This information can be obtained only by direct *folding* simulations.